Preprint number: J-PARC-TH-0138, KYUSHU-HET-190, RIKEN-QHP-???

Thermodynamics in the quenched QCD —EMT with NNLO gradient flow coefficients—

Takumi Iritani[1] Masakiyo Kitazawa[2,3] Hiroshi Suzuki[4,*] Hiromasa Takaura[4]

[1] *Theoretical Research Division, Nishina Center, RIKEN, Wako 351-0198, Japan*
[2] *Department of Physics, Osaka University, Toyonaka, Osaka 560-0043, Japan*
[3] *J-PARC Branch, KEK Theory Center, Institute of Particle and Nuclear Studies, KEK, 203-1, Shirakata, Tokai, Ibaraki, 319-1106, Japan*
[4] *Department of Physics, Kyushu University 744 Motooka, Nishi-ku, Fukuoka, 819-0395, Japan*
[*] *E-mail: hsuzuki@phys.kyushu-u.ac.jp*

25/10/2018

Recently, Harlander, Kluth, and Lange computed the two-loop order (i.e., NNLO) coefficients in the gradient flow representation of the energy–momentum tensor (EMT) in vector-like gauge theories. In this paper, we study the effect of the two-loop order corrections (and the three-loop order correction for the trace part of the EMT that is available through the trace anomaly) on the lattice computation of thermodynamic quantities in the quenched QCD. The use of the two-loop order coefficients generally reduces the t dependence of the expectation value of relevant flowed operators, where t is the flow time. We argue that this tendency can be naturally understood as the reduction of the perturbative error contained in the one-loop order coefficients. With the use of the two-loop order coefficients, therefore, the $t \to 0$ extrapolation becomes less sensitive on the fit function, the fit range, and the choice of the renormalization scale; the systematic error associated with these factors is considerably reduced.

Subject Index B01, B31, B32, B38

1. Introduction and the summary

The energy–momentum tensor (EMT) $T_{\mu\nu}(x)$ is a fundamental physical observable in quantum field theory. It has been pointed out in Refs. [1, 2] that a "universal" representation of the EMT can be written down if one utilizes the so-called gradient flow [3–7] and its small flow time expansion [6]. This representation of the EMT is universal in the sense that it is independent of the adopted regularization. The representation can thus be employed in particular with the lattice regularization that makes nonperturbative computations possible. An advantage of this approach to the lattice EMT is that the expression of the EMT is known a priori and it is not necessary to compute the renormalization constants involved in the lattice EMT [8].[1] This approach instead requires the limit $t \to 0$, where t is the flow time (see below), because the representation is obtained in the small flow time limit. In actual lattice simulations, however, since t is limited as $t \gtrsim a^2$ by the lattice spacing a, the $t \to 0$ limit requires the extrapolation for $t \to 0$; this $t \to 0$ extrapolation can be a source of the systematic error. By employing this gradient flow representation of the EMT, expectation values and correlation functions of the EMT have been computed to study various physical questions [12–20].

One of important applications of the lattice EMT is the thermodynamics of gauge theory at finite temperature. See Refs. [21–25] and more recent works in Refs. [26–31]. Both of two independent thermodynamic quantities, such as the energy density ε and the pressure p, can be directly computed as the finite temperature expectation value of the traceless part and the trace part of the EMT, respectively. That is,[2]

$$\varepsilon + p = -\frac{4}{3}\left\langle T_{00}(x) - \frac{1}{4}T_{\mu\nu}(x)\right\rangle, \tag{1.1}$$

$$\varepsilon - 3p = -\left\langle T_{\mu\mu}(x)\right\rangle. \tag{1.2}$$

In the gradient flow approach, moreover, the computation of isotropic/anisotropic Karsch coefficients (i.e., the lattice β function) is also not necessary, because the expression of the EMT is a priori known.

In this paper, we consider the thermodynamics in the quenched QCD, i.e., the pure Yang–Mills theory. Assuming the dimensional regularization, the EMT in the pure Yang–Mills theory is given by

$$T_{\mu\nu}(x) = \frac{1}{g_0^2}\left[F^a_{\mu\rho}(x)F^a_{\nu\rho}(x) - \frac{1}{4}\delta_{\mu\nu}F^a_{\rho\sigma}(x)F^a_{\rho\sigma}(x)\right], \tag{1.3}$$

where g_0 is the bare gauge coupling and $F^a_{\mu\nu}(x) \equiv \partial_\mu A^a_\nu(x) - \partial_\nu A^a_\mu(x) + f^{abc}A^b_\mu(x)A^c_\nu(x)$ is the field strength.[3] Note that this is an expression in the $D \equiv 4 - 2\epsilon$ dimensional spacetime and is not generally traceless.

One can express any composite operator in gauge theory such as the EMT (1.3) as a series of flowed composite operators through the small flow time expansion [6]. That is, one can

[1] See a review [9] and references cited therein. In particular, in Refs. [10, 11], the gradient flow is applied to the construction of the EMT in the conventional approach [8].

[2] For simplicity of expression, here and in what follows we omit the subtraction of the vacuum expectation value of an expression; this is always assumed.

[3] f^{abc} denote the structure constants of the gauge group G.

write[4]

$$T_{\mu\nu}(x) = c_1(t)\left[G^a_{\mu\rho}(t,x)G^a_{\nu\rho}(t,x) - \frac{1}{4}\delta_{\mu\nu}G^a_{\rho\sigma}(t,x)G^a_{\rho\sigma}(t,x)\right] + c_2(t)\delta_{\mu\nu}G^a_{\rho\sigma}(t,x)G^a_{\rho\sigma}(t,x) + O(t), \tag{1.4}$$

where $G^a_{\mu\nu}(t,x) \equiv \partial_\mu B^a_\nu(t,x) - \partial_\nu B^a_\mu(t,x) + f^{abc}B^b_\mu(t,x)B^c_\nu(t,x)$ and $D_\nu G^a_{\nu\mu}(t,x) \equiv \partial_\nu G^a_{\nu\mu}(t,x) + f^{abc}B^b_\nu(t,x)G^c_{\nu\mu}(t,x)$. In these expressions, the "flowed" gauge field $B^a_\mu(t,x)$ is defined by the gradient flow [3–5], i.e., a one-parameter evolution of the original gauge field by

$$\partial_t B^a_\mu(t,x) = D_\nu G^a_{\nu\mu}(t,x), \qquad B^a_\mu(t=0,x) = A^a_\mu(x). \tag{1.5}$$

The parameter $t \geq 0$, which possesses the mass dimension -2, is termed the flow time. Since Eq. (1.4) is finite [6], one can set $D = 4$ and the first term in the right-hand side that is proportional to $c_1(t)$ is traceless. The coefficients in this small flow time expansion, which are analogous to the Wilson coefficients in OPE, can be calculated by perturbation theory [6], as

$$c_1(t) = \frac{1}{g^2}\sum_{\ell}^{\infty} k_1^{(\ell)}\left[\frac{g^2}{(4\pi)^2}\right]^\ell, \qquad c_2(t) = \frac{1}{g^2}\sum_{\ell=1}^{\infty} k_2^{(\ell)}\left[\frac{g^2}{(4\pi)^2}\right]^\ell, \tag{1.6}$$

where g denotes the renormalized gauge coupling. For this, throughout this paper, we assume the $\overline{\rm MS}$ scheme, in which

$$g_0^2 = \left(\frac{\mu^2 e^{-\gamma_E}}{4\pi}\right)^\epsilon g^2 Z_g, \tag{1.7}$$

where μ is the renormalization scale, γ_E is the Euler constant, and Z_g is the renormalization factor. In Eq. (1.6),

$$k_1^{(0)} = 1, \tag{1.8}$$

because in the tree level (i.e., LO) approximation, $F^a_{\mu\rho}(x)F^a_{\nu\rho}(x) = G^a_{\mu\rho}(t,x)G^a_{\nu\rho}(t,x) + O(t)$. On the other hand, there is no "$k_2^{(0)}$" in Eq. (1.6) because the EMT is traceless in the tree level approximation (the trace anomaly emerges from the one-loop order).

In Eq. (1.6), the one-loop order (i.e., NLO) coefficients $k_i^{(1)}(t)$ ($i = 1, 2$) were computed in Refs. [1, 2] (see also Ref. [33]). Recently, in Ref. [32], Harlander, Kluth, and Lange computed the two-loop order (i.e., NNLO) coefficients $k_i^{(2)}(t)$ for general vector-like gauge theories. See also Ref. [34]. The purpose of the present paper is to study the effect of the two-loop corrections given in Ref. [32] by taking the lattice computation of thermodynamic quantities in the quenched QCD as example. For the trace part of the EMT, we also examine the use of the three-loop order coefficient, $k_2^{(3)}$; as we will explain below, for the quenched QCD, this higher order coefficient can be obtained by combining a two-loop result in Ref. [32] and the trace anomaly [35–37]. From analyses by using lattice data obtained in Ref. [14], we find that the use of the two-loop order coefficients generally reduces the t dependence of the expectation value of relevant flowed operators, where t is the flow time. We argue that this tendency can be naturally understood as the reduction of the perturbative error contained in the one-loop order coefficient. This understanding is obtained by a careful analysis of the asymptotic behavior of relevant flowed operators for $t \to 0$ (Sect. 3). With the use of

[4] Note that our convention for $c_2(t)$ differ from that of Ref. [32]. Our $c_2(t)$ corresponds to $c_2(t) + (1/4)c_1(t)$ in Ref. [32].

the two-loop order coefficients, therefore, the $t \to 0$ extrapolation becomes less sensitive on the fit function, the fit range, and the choice of the renormalization scale; the systematic error associated with these factors is considerably reduced. We expect that this improvement brought about by the two-loop order coefficients persists also in wider applications of the gradient flow representation of the EMT, such as the thermodynamics of the full QCD.

2. Expansion coefficients

2.1. β function and the running gauge coupling constant

The β function corresponding to Eq. (1.7) is given by

$$\beta(g) \equiv \mu \frac{\partial}{\partial \mu} g \Big|_{g_0} \overset{\epsilon \to 0}{\to} -g \sum_{\ell=1}^{\infty} \beta_{\ell-1} \left[\frac{g^2}{(4\pi)^2} \right]^{\ell}, \tag{2.1}$$

with coefficients [38–44]

$$\beta_0 = \frac{11}{3} C_A, \tag{2.2}$$

$$\beta_1 = \frac{34}{3} C_A^2, \tag{2.3}$$

$$\beta_2 = \frac{2857}{54} C_A^3, \tag{2.4}$$

$$\beta_3 = \left[\frac{150473}{486} + \frac{44}{9} \zeta(3) \right] C_A^4 + \left[-\frac{40}{3} + 352 \zeta(3) \right] C_A^2, \tag{2.5}$$

where C_A is the quadratic Casimir for the adjoint representation,

$$f^{acd} f^{bcd} = C_A \delta^{ab}. \tag{2.6}$$

$C_A = N$ for the gauge group $G = SU(N)$.

Now, to compute correlation functions of the EMT by employing the representation (1.4), one has to take the limit $t \to 0$ [1, 2]. First of all this limit removes the last $O(t)$ term in Eq. (1.4), the contribution of operators of higher (≥ 6) mass dimensions. Also, to justify finite order truncation of the perturbative expansion (1.6), one invokes the following renormalization group argument [1, 2]: The EMT (1.3) and the operator $G^a_{\mu\rho}(t,x) G^a_{\nu\rho}(t,x)$ are bare quantities. Then the coefficients $c_i(t)$ ($i = 1, 2$) in Eq. (1.4) are independent of the renormalization scale μ (when the bare coupling g_0 is kept fixed). One then set $\mu \propto 1/\sqrt{t}$ and concurrently replaces the coupling constant g with the running gauge coupling $g(\mu)$ satisfying

$$\mu \frac{dg(\mu)}{d\mu} = \beta(g(\mu)). \tag{2.7}$$

Then the use of the perturbative calculation is justified for small t because the running gauge coupling $g(\mu)$ gets smaller due to the asymptotic freedom.

Although the above argument shows that in principle the coefficients $c_i(t)$ are independent of the choice of the relation between the renormalization scale μ and the flow time t, this is not exactly the case in practical calculations based on fixed order perturbation theory. In other words, the difference caused by different choices of μ implies the remaining perturbative

uncertainty. Following Ref. [32], we introduce the combination,

$$L(\mu, t) \equiv \ln(2\mu^2 t) + \gamma_E. \tag{2.8}$$

A conventional choice of μ is given by

$$\mu = \mu_d(t) \equiv \frac{1}{\sqrt{8t}} \Leftrightarrow L = -2\ln 2 + \gamma_E. \tag{2.9}$$

All the numerical experiments on the basis of the representation (1.4) so far [12–20] have adopted this choice. On the other hand, in Ref. [32], it is argued that

$$\mu = \mu_0(t) \equiv \frac{1}{\sqrt{2e^{\gamma_E} t}} \Leftrightarrow L = 0, \tag{2.10}$$

would be an optimal choice on the basis of the two-loop order coefficients. In following numerical analyses, we will examine both choices $\mu = \mu_0(t)$ and $\mu = \mu_d(t)$. The difference in the results with these two choices gives an estimate of higher order uncertainty. We define our central values by the usage of Eq. (2.10), while the higher order uncertainties are estimated with Eq. (2.9), where $\mu_d(t) \simeq 0.667\mu_0(t)$.

Let us now list the known coefficients in Eq. (1.6).

2.2. One-loop order (NLO) coefficients

In the one-loop level, we have [1, 2, 33]

$$\begin{aligned} k_1^{(1)} &= -\beta_0 L - \frac{7}{3} C_A \\ &= C_A \left(-\frac{11}{3} L - \frac{7}{3} \right). \end{aligned} \tag{2.11}$$

$$\begin{aligned} k_2^{(1)} &= \frac{1}{8}\beta_0 \\ &= \frac{11}{24} C_A. \end{aligned} \tag{2.12}$$

The number L is defined by Eq. (2.8).

2.3. Two-loop order (NNLO) coefficients

he two-loop order coefficients in Ref. [32] specialized to the pure Yang–Mills theory are

$$\begin{aligned} k_1^{(2)} &= -\beta_1 L + C_A^2 \left(-\frac{14482}{405} - \frac{16546}{135}\ln 2 + \frac{1187}{10}\ln 3 \right) \\ &= C_A^2 \left(-\frac{34}{3} L - \frac{14482}{405} - \frac{16546}{135}\ln 2 + \frac{1187}{10}\ln 3 \right). \end{aligned} \tag{2.13}$$

$$\begin{aligned} k_2^{(2)} &= \frac{1}{8}\beta_1 - \frac{7}{16}\beta_0 C_A \\ &= C_A^2 \left(-\frac{3}{16} \right). \end{aligned} \tag{2.14}$$

2.4. Three-loop order (N^3LO) coefficient for $c_2(t)$, $k_2^{(3)}$

In the pure Yang–Mills theory, if one has the small flow time expansion of the renormalized operator $\{F^a_{\mu\nu}F^a_{\mu\nu}\}_R(x)$ in the ℓth loop order, one can further obtain the coefficient of $c_2(t)$ in

a one loop higher, $k_2^{(\ell+1)}$, by using information of the trace anomaly [1]. The two-loop order (NNLO) coefficient (2.14) can also be obtained in this way from a one-loop order calculation and already has been used in numerical experiments in the quenched QCD. Repeating this argument, we can now obtain the three-loop order coefficient, $k_2^{(3)}$.

We recall the trace anomaly [35–37]

$$T_{\mu\mu}(x) = -\frac{\beta(g)}{2g^3}\{F^a_{\mu\nu}F^a_{\mu\nu}\}_R(x), \tag{2.15}$$

where the β function given by Eq. (2.1). According to Eq. (64) of Ref. [32], we now have the small flow time expansion of $\{F^a_{\mu\nu}F^a_{\mu\nu}\}_R(x)$ to the two-loop order:

$$\begin{aligned}
&\{F^a_{\mu\nu}F^a_{\mu\nu}\}_R(x) \\
&= \left[1 + \frac{g^2}{(4\pi)^2}\left(-\frac{7}{2}C_A\right) + \frac{g^4}{(4\pi)^4}C_A^2\left(-\frac{3}{2}L - \frac{1427}{180} + \frac{87}{5}\ln 2 - \frac{54}{5}\ln 3\right)\right] \\
&\quad \times G^a_{\mu\nu}(t,x)G^a_{\mu\nu}(t,x) + O(t).
\end{aligned} \tag{2.16}$$

Plugging this into Eq. (2.15) and using (2.1), we have

$$\begin{aligned}
&T_{\mu\mu}(x) \\
&= \frac{1}{g^2}\left\{\frac{g^2}{(4\pi)^2}\frac{1}{2}\beta_0 + \frac{g^4}{(4\pi)^4}\left(\frac{1}{2}\beta_1 - \frac{7}{4}\beta_0 C_A\right)\right. \\
&\qquad \left. + \frac{g^6}{(4\pi)^6}\left[\frac{1}{2}\beta_2 - \frac{7}{4}\beta_1 C_A + \beta_0 C_A^2\left(-\frac{3}{4}L - \frac{1427}{360} + \frac{87}{10}\ln 2 - \frac{54}{10}\ln 3\right)\right]\right\} \\
&\qquad \times G^a_{\mu\nu}(t,x)G^a_{\mu\nu}(t,x) + O(t).
\end{aligned} \tag{2.17}$$

Comparing this with the trace of Eq. (1.4), we have Eqs. (2.12) and (2.14), and

$$\begin{aligned}
k_2^{(3)} &= \frac{1}{8}\beta_2 - \frac{7}{16}\beta_1 C_A + \beta_0 C_A^2\left(-\frac{3}{16}L - \frac{1427}{1440} + \frac{87}{40}\ln 2 - \frac{27}{20}\ln 3\right) \\
&= C_A^3\left(-\frac{11}{16}L - \frac{2849}{1440} + \frac{319}{40}\ln 2 - \frac{99}{20}\ln 3\right).
\end{aligned} \tag{2.18}$$

We will also examine the use of this N^{3}LO coefficient for the trace anomaly in the numerical analyses below.

3. Asymptotic behavior for $t \to 0$

As already elucidated, to compute expectation values and correlation functions of the EMT by employing the representation (1.4), one has to take the $t \to 0$ limit. In actual numerical calculations based on the lattice simulation, however, it is not straightforward to take the $t \to 0$ limit. The representation (1.4) assumes a continuous spacetime and one has to take a double limit, i.e., the continuum limit $a \to 0$ first while the flow time t in physical units is kept fixed and then the $t \to 0$ limit. In other words, with a finite lattice spacing a, the flow time t is practically limited from below as $t \gtrsim a^2$ (the lattice data actually exhibits violent diverging behavior for $t \lesssim a^2$). Then one has to carry out extrapolation for $t \to 0$ by assuming a certain functional form. For this $t \to 0$ extrapolation, therefore, it is quite

desirable to know the $t \to 0$ behavior of the combination,

$$c_1^{(\ell)}(t) \left[G^a_{\mu\rho}(t,x) G^a_{\nu\rho}(t,x) - \frac{1}{4} \delta_{\mu\nu} G^a_{\rho\sigma}(t,x) G^a_{\rho\sigma}(t,x) \right] + c_2^{(\ell)}(t) \delta_{\mu\nu} G^a_{\rho\sigma}(t,x) G^a_{\rho\sigma}(t,x), \quad (3.1)$$

where $c_i^{(\ell)}(t)$ denote the ℓth loop order truncation of the coefficients $c_i(t)$:

$$c_1^{(\ell)}(t) \equiv \frac{1}{g^2} \sum_{n=0}^{\ell} k_1^{(n)} \left[\frac{g^2}{(4\pi)^2} \right]^n, \qquad c_2^{(\ell)}(t) \equiv \frac{1}{g^2} \sum_{n=1}^{\ell} k_2^{(n)} \left[\frac{g^2}{(4\pi)^2} \right]^n. \quad (3.2)$$

At first glance, this appears an impossible task because the matrix elements of $G^a_{\mu\rho}(t,x) G^a_{\nu\rho}(t,x)$ can have quite nontrivial t dependence. For this reason, in numerical experiments so far, the extrapolation by the linear function in t, which is suggested by the presence of the last $O(t)$ term of Eq. (1.4) has been mainly used. Here, we point out that it is possible to argue the asymptotic $t \to 0$ behavior of Eq. (3.1) in a theoretically solid basis. *If* the flow time available in numerical simulations can be considered to be "sufficiently small" in the sense elucidated below, one should use the following asymptotic form in the $t \to 0$ extrapolation.

We first take the traceless (TL) part of Eq. (1.4), which yields

$$T^{TL}_{\mu\nu}(x) = c_1(t) \left[G^a_{\mu\rho}(t,x) G^a_{\nu\rho}(t,x) - \frac{1}{4} \delta_{\mu\nu} G^a_{\rho\sigma}(t,x) G^a_{\rho\sigma}(t,x) \right] + O(t). \quad (3.3)$$

Multiplying this by $c_1^{(\ell)}(t) c_1(t)^{-1}$, we have

$$c_1^{(\ell)}(t) \left[G^a_{\mu\rho}(t,x) G^a_{\nu\rho}(t,x) - \frac{1}{4} \delta_{\mu\nu} G^a_{\rho\sigma}(t,x) G^a_{\rho\sigma}(t,x) \right] = c_1^{(\ell)}(t) c_1(t)^{-1} T^{TL}_{\mu\nu}(x) + O(t). \quad (3.4)$$

Now, since $T^{TL}_{\mu\nu}(x)$ *is* independent of the flow time t., the combination $c_1^{(\ell)}(t) c_1(t)^{-1}$ provides the t dependence of the left-hand side up to the last $O(t)$ term. $c_1^{(\ell)}(t) c_1(t)^{-1}$ is almost unity up to the perturbative error of the order

$$\left[\frac{g(\mu)^2}{(4\pi)^2} \right]^{\ell+1} \overset{t\to 0}{\sim} \frac{1}{[\beta_0 \ln(\mu^2/\Lambda^2_{\overline{\rm MS}})]^{\ell+1}}, \quad (3.5)$$

where we have used the leading $\mu \to \infty$ form of the running coupling; recall that the renormalization scale μ and the flow time t are related by Eq. (2.8), i.e.,

$$\mu = \frac{1}{\sqrt{2e^{-L+\gamma_E} t}}. \quad (3.6)$$

In the limit $t \to 0$, the $1/[-\ln(t\Lambda^2_{\overline{\rm MS}})]^{\ell+1}$ behavior of Eq. (3.5) is always dominant over any power of t, $t^k \sim \exp\{-(4\pi)^2 k/[\beta_0 g(\mu)^2]\}$. Therefore, for $t \to 0$, in the mathematical sense, the last $O(t)$ term in Eq. (3.4) is negligible compared with Eq. (3.5) and the leading asymptotic behavior of Eq. (3.4) in the limit $t \to 0$ is

$$\begin{aligned} & c_1^{(\ell)}(t) \left[G^a_{\mu\rho}(t,x) G^a_{\nu\rho}(t,x) - \frac{1}{4} \delta_{\mu\nu} G^a_{\rho\sigma}(t,x) G^a_{\rho\sigma}(t,x) \right] \\ & = c_1^{(\ell)}(t) c_1(t)^{-1} T^{TL}_{\mu\nu}(x) + O(t) \\ & \overset{t\to 0}{\sim} T^{TL}_{\mu\nu}(x) \left\{ 1 + s_1 \left[\frac{g(\mu)^2}{(4\pi)^2} \right]^{\ell+1} \right\}, \end{aligned} \quad (3.7)$$

where s_1 is a constant and the renormalization scale μ is given by Eq. (3.6).[5] From Eqs. (1.6), (3.2), and (2.13), we have

$$s_1 = -k_1^{(2)} = -87.24 \qquad \text{for } \ell = 1 \text{ (NLO)}, \tag{3.8}$$

$$s_1 = -k_1^{(3)} \qquad \text{for } \ell = 2 \text{ (NNLO)}, \tag{3.9}$$

where the explicit number quoted for $\ell = 1$ is for $G = SU(3)$ and $\mu = \mu_0$, i.e., $L = 0$.

A similar argument for the trace part of Eq. (1.4) yields[6]

$$\begin{aligned} & 4c_2^{(\ell)}(t) G^a_{\mu\nu}(t,x) G^a_{\mu\nu}(t,x) \\ & = c_2^{(\ell)}(t) c_2(t)^{-1} T_{\mu\mu}(x) + O(t) \\ & \overset{t\to 0}{\sim} T_{\mu\mu}(x) \left\{ 1 + s_2 \left[\frac{g(\mu)^2}{(4\pi)^2} \right]^\ell \right\}, \end{aligned} \tag{3.10}$$

where s_2 is another constant. Again, from Eqs. (1.6), (3.2), (2.12), (2.14), and (2.18),

$$s_2 = -\frac{k_2^{(2)}}{k_2^{(1)}} \simeq 1.227 \qquad \text{for } \ell = 1 \text{ (NLO)}, \tag{3.11}$$

$$s_2 = -\frac{k_2^{(3)}}{k_2^{(1)}} \simeq 37.09 \qquad \text{for } \ell = 2 \text{ (NNLO)}, \tag{3.12}$$

$$s_2 = -\frac{k_2^{(4)}}{k_2^{(1)}} \qquad \text{for } \ell = 3 \text{ (N}^3\text{LO)}. \tag{3.13}$$

If the flow time t is sufficiently small such that the $O(t)$ terms in the above expressions are negligible compared with the perturbative error $[g^2/(4\pi)^2]^\ell$, the asymptotic behavior of Eq. (3.1) for $t \to 0$ is given by Eqs. (3.7)–(3.13). Whether t available in actual lattice experiments can be regarded so small or not depends on lattice parameters such as the lattice spacing, physical parameters such as $\Lambda_{\overline{\rm MS}}$, the temperature and the volume, and also on a physical quantity under consideration; this is because the above $O(t)$ terms contain higher dimensional operators whose matrix elements depend on these factors.

In the numerical analyses in the next section for thermodynamic quantities, we use two reasonable fit ranges for the $t \to 0$ extrapolation [14],

$$\text{Range-1: } 0.01 \le tT \le 0.015, \tag{3.14}$$

$$\text{Range-2: } 0.005 \le tT \le 0.015. \tag{3.15}$$

In Fig. 1, we plot $t\Lambda^2_{\overline{\rm MS}}$ and $g(\mu)^4/(4\pi)^4$, as a function of tT^2 for various temperature T (T_c denotes the critical temperature) adopting $\mu = \mu_0(t)$ (2.10).[7] We observe that within our fitting range, $t\Lambda^2_{\overline{\rm MS}} \sim 30 g(\mu)^4/(4\pi)^4$. By considering the fact that the parameter s_1 in Eq. (3.8) and the parameter s_2 in Eq. (3.12) are ~ -90 and ~ 40, respectively, the

[5] In this expression, it is natural to use the running gauge coupling $g(\mu)$ in the ℓth loop order.

[6] The power is ℓ instead of $\ell + 1$, because the series (1.6) for $c_2(t)$ starts from g^2, not g^0.

[7] Throughout this paper, we use three-loop $\Lambda_{\overline{\rm MS}}$ quoted in Eq. (270) of Ref. [45] and the four-loop running gauge coupling in the $\overline{\rm MS}$ scheme. For the latter, we use the approximate formula, Eq. (9.5) in Ref. [46].

t dependences arising from $g(\mu)^4/(4\pi)^4$ and $t\Lambda^2_{\overline{\rm MS}}$ can be comparable within the above range. In the next section, we will see that numerical results strongly indicate that the t dependence in Eq. (3.7) in the $\ell = 1$ (NLO) is dominated by $g(\mu)^4/(4\pi)^4$ rather than the $O(t)$ term. Nevertheless, for other cases, it is not obvious which factor is dominant. Therefore, unfortunately, we cannot strongly insist the $t \to 0$ extrapolation on the basis of the asymptotic behaviors (3.7) and (3.10). It will be safe if one tries both the "traditional" extrapolation by the linear function in t and the extrapolation of the forms (3.7) and (3.10). The difference in the $t \to 0$ limit should be regarded as the systematic error associated with the $t \to 0$ extrapolation; we will find that the new two-loop order (NNLO) coefficients considerably reduces this error.

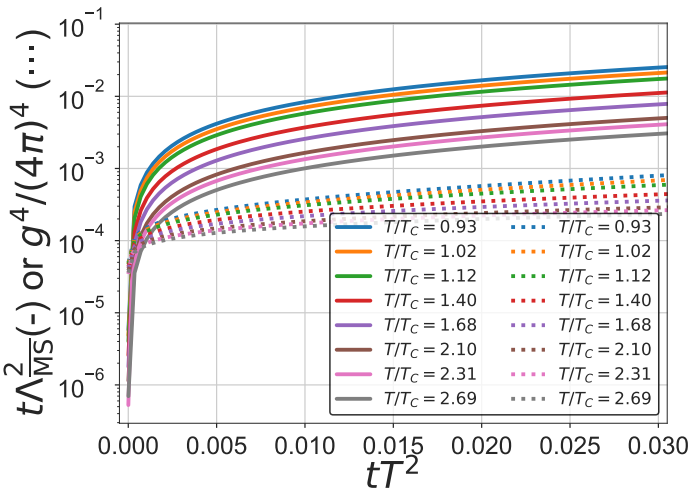

Fig. 1: $t\Lambda^2_{\overline{\rm MS}}$ and $g(\mu)^4/(4\pi)^4$ as a function of tT^2 for various temperature T (T_c denotes the critical temperature). Here, we adopt $\mu = \mu_0(t)$ (2.10)).

4. Numerical results

In what follows, we use the lattice data obtained in Ref. [14] for the $G = SU(3)$ pure Yang–Mills theory, which allows detailed analyses.

Let us start with the entropy density, $\varepsilon + p$. In Fig. 2, we plot the the thermal expectation value

$$-\frac{4}{3T^4}c_1(t)\left\langle G^a_{0\rho}(t,x)G^a_{0\rho}(t,x) - \frac{1}{4}G^a_{\rho\sigma}(t,x)G^a_{\rho\sigma}(t,x)\right\rangle, \tag{4.1}$$

as a function of tT^2; the temperature is $T/T_c = 1.68$. The plots for other temperatures listed in the left most column of Table 1 are deferred to Appendix A.

According to Eqs. (1.4) and (1.1), the $t \to 0$ limit of this expectation value gives rise to the entropy density normalized by the temperature, $(\varepsilon + p)/T^4$. In each panel of Fig. 2, we plot Eq. (4.1) with three different lattice spacings; the coefficient $c_1(t)$ in each panel is, (a) the one-loop order (i.e., NLO) with the choice of the renormalization scale $\mu_0(t)$ (2.10), (b) the NLO with $\mu_d(t)$ (2.9), (c) the two-loop order (i.e., NNLO or N^{2}LO) with $\mu_0(t)$, and (d) the N^{2}LO perturbation theory with $\mu_d(t)$, respectively. We then take the continuum limit at

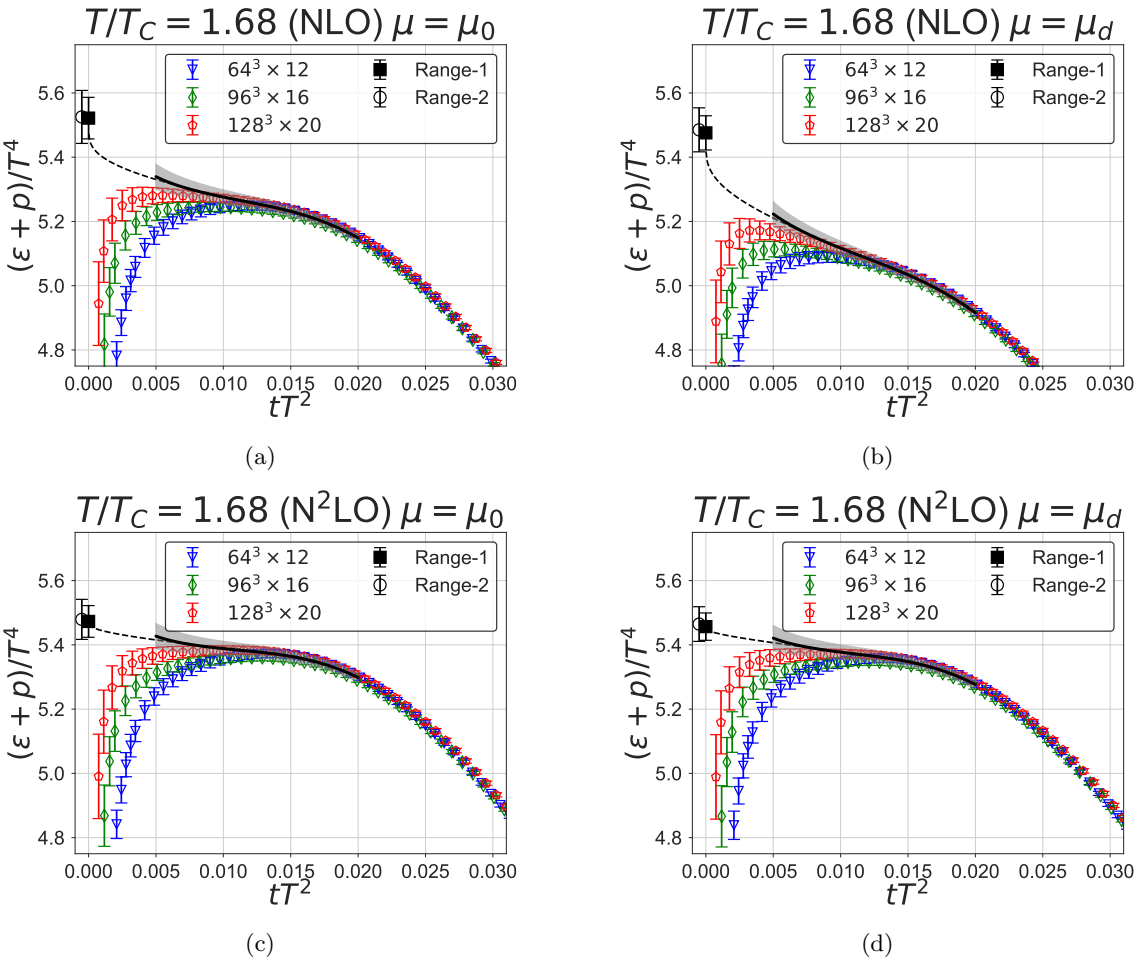

Fig. 2: Equation (4.1) as the function of tT^2. $T = 1.68T_c$. In each panel, the order of perturbation theory and the choice of the renormalization scale are indicated. The errors are statistical only. The extrapolation of the continuum limit (the gray band) to $t = 0$ is plotted by the black circle (obtained by the fit range (3.14)) and the white circle (obtained by the fit range (3.15)).

each fixed value of tT^2. The continuum limit (the gray band) is then extrapolated to $t = 0$ by the fit of the form of the right-hand side of Eq. (3.7); $\ell = 1$ for NLO and $\ell = 2$ for N^{2}LO. We summarize the values of the slope parameter s_1 in Table 2.

In Fig. 2 and in corresponding figures in Appendix A, Fig. A1–A7, we observe that the use of the two-loop order coefficient generally reduces the t dependence of the continuum limit (it becomes flatter in t). This implies that the $t \to 0$ extrapolation becomes less sensitive on the fit function, the fit range, and the choice of the renormalization scale.[8] This tendency can be naturally understood from the asymptotic behavior for $t \to 0$ in Eqs. (3.7) and (3.8) if we assume that the t-dependence with the one-loop order (NLO) coefficient is mainly determined by the $g(\mu)^4/(4\pi)^4$ term compared with the $O(t)$ term. If this is the case, then the

[8] The reduction of the renormalization scale dependence from the one-loop order to the two-loop order is studied in detail in Ref. [32].

$(\varepsilon+p)/T^4$			
T/T_c	NLO	N^{2}LO	FlowQCD 2016
0.93	0.077(47)(00)(00)(05)	0.082(38)(00)(00)(04)	0.082(33)$(^{+3}_{-6})$(0)
1.02	2.185(75)(00)(15)(35)	2.169(68)(02)(22)(09)	2.104(63)$(^{+16}_{-2})$(8)
1.12	3.711(69)(14)(22)(22)	3.708(55)(10)(34)(04)	3.603(46)$(^{+39}_{-0})$(13)
1.40	4.849(60)(00)(26)(16)	4.846(47)(00)(40)(05)	4.706(35)$(^{+49}_{-0})$(17)
1.68	5.522(65)(04)(31)(46)	5.473(49)(06)(44)(16)	5.285(35)$(^{+44}_{-0})$(18)
2.10	5.811(67)(00)(28)(24)	5.784(50)(00)(41)(06)	5.617(34)$(^{+66}_{-0})$(18)
2.31	5.786(109)(00)(25)(03)	5.790(82)(00)(39)(06)	5.657(55)$(^{+82}_{-15})$(18)
2.69	6.161(70)(13)(29)(36)	6.106(52)(13)(41)(15)	5.914(32)$(^{+70}_{-0})$(18)
$(\varepsilon-3p)/T^4$			
T/T_c	N^{2}LO	N^{3}LO	FlowQCD 2016
0.93	0.054(41)(00)(01)(10)	0.064(34)(00)(00)(06)	0.066(32)$(^{+3}_{-2})$(0)
1.02	1.927(62)(00)(01)(14)	1.933(58)(00)(00)(03)	1.945(57)$(^{+8}_{-7})$(0)
1.12	2.535(42)(00)(01)(18)	2.544(35)(00)(00)(04)	2.560(33)$(^{+12}_{-8})$(0)
1.40	1.767(38)(00)(00)(05)	1.769(29)(00)(00)(00)	1.777(24)$(^{+14}_{-3})$(0)
1.68	1.220(31)(13)(00)(06)	1.207(24)(10)(00)(06)	1.201(19)$(^{+10}_{-0})$(0)

Table 1: Summary of the entropy density and the trace anomaly obtained by using coefficients in different orders of perturbation theory. The central values and the statistical errors (the 1st parentheses) are computed by using the Range-1 (3.14) with the choice of the renormalization scale $\mu = \mu_0(t)$ (2.10). The numbers in the 2nd, the 3rd, and the 4th parentheses are the systematic errors associated with the fit range (estimated by another choice, the Range-2 (3.15), the 3% uncertainty of $\Lambda_{\overline{\rm MS}}$, and the renormalization scale (estimated from another choice $\mu = \mu_d(t)$ (2.9)), respectively. The results of Ref. [14] are also tabulated in the last column.

t-dependence diminishes when we increase the order of loop approximation. Another support on this picture is provided that the fact that the values of s_1 in Table 2, the slope parameter in Eq. (3.7), obtained by the fit is fairly consistent with -87.24 in Eq (3.8). For N^{2}LO, on the other hand, we do not have a clear idea which of the $g(\mu)^6/(4\pi)^6$ term and the $O(t)$ term dominates the t dependence. In any case, we cannot be completely sure which the perturbative error $\propto [g(\mu)^2/(4\pi)^2]^{\ell+1}$ and the (nonperturbative) $O(t)$ term dominates the t dependence. We should use (at least) both the linear function in t and the functional form in Eq. (3.7) for the $t \to 0$ extrapolation. The difference in the $t \to 0$ limit should be regarded as the systematic error associated with the $t \to 0$ extrapolation. See Table 1 and Fig. 3 for the summary of the results. In these results, for one-loop order (NLO) cases, we used the extrapolation of the form (3.7). The linear t extrapolation was adopted in Ref. [14]. Thus the different between these two is regarded as the systematic error in the NLO. For two-loop order (N^{2}LO), we examined both the extrapolation of the form (3.7) and the linear t extrapolation and the difference is included in the systematic error; we found that the fit by the sum of these two functions is unstable because the continuum limit is almost linear in t. However, because of the reduction of the t dependence with the two-loop coefficient,

s_1		
T/T_c	NLO ($\ell=1$)	N^{2}LO ($\ell=2$)
0.93	$398(1239)(^{+426}_{+0})(^{+80}_{-71})$	$16503(38219)(^{+13877}_{+0})(^{+2775}_{-2452})$
1.02	$-152(42)(^{+0}_{+0})(^{+26}_{-23})$	$-1902(1574)(^{+0}_{-120})(^{+966}_{-834})$
1.12	$-95(34)(^{+0}_{-11})(^{+32}_{-28})$	$185(1299)(^{+0}_{-430})(^{+1224}_{-1073})$
1.40	$-96(33)(^{+3}_{+0})(^{+33}_{-30})$	$160(1377)(^{+122}_{+0})(^{+1415}_{-1256})$
1.68	$-202(36)(^{+0}_{-3})(^{+28}_{-26})$	$-4717(1653)(^{+0}_{-317})(^{+1265}_{-1123})$
2.10	$-159(43)(^{+3}_{+0})(^{+33}_{-30})$	$-2965(2141)(^{+34}_{+0})(^{+1617}_{-1455})$
2.31	$-79(76)(^{+54}_{+0})(^{+39}_{-36})$	$1056(3835)(^{+2792}_{+0})(^{+1971}_{-1785})$
2.69	$-251(51)(^{+0}_{-12})(^{+31}_{-29})$	$-8193(2771)(^{+0}_{-935})(^{+1618}_{-1460})$
s_2		
T/T_c	N^{2}LO ($\ell=2$)	N^{3}LO ($\ell=3$)
0.93	$1216(2116)(^{+120}_{+0})(^{+93}_{-86})$	$31549(46881)(^{+5673}_{+0})(^{+2954}_{-2695})$
1.02	$60(31)(^{+14}_{+0})(^{+5}_{-4})$	$669(1020)(^{+534}_{+0})(^{+173}_{-158})$
1.12	$69(28)(^{+14}_{+0})(^{+5}_{-5})$	$1027(987)(^{+589}_{+0})(^{+193}_{-177})$
1.40	$44(57)(^{+9}_{+0})(^{+3}_{-3})$	$193(2219)(^{+366}_{+0})(^{+131}_{-120})$
1.68	$-98(73)(^{+0}_{-44})(^{+3}_{-3})$	$-5883(3170)(^{+0}_{-2214})(^{+186}_{-197})$

Table 2: The slope parameters s_1 in Eq. (3.7) and s_2 in Eq. (3.10) obtained from the fit of the continuum limit. The renormalization scale $\mu=\mu_0(t)$ (2.10) is adopted. The central value is obtained from the fit in the Range-1 (3.14). Each parentheses show the statistical error, the systematic error associated with the fit range (estimated by another choice, the Range-2 (3.15), and the systematic error associated with the the 3% uncertainty of $\Lambda_{\overline{\rm MS}}$.

the systematic error in N^{2}LO is much small. This clearly shows a great advantage of the two-loop order coefficient.

In Fig. 3, we also the results of Refs. [14, 21, 23, 29, 31]. That our N^{2}LO results are consistent with other references, especially with Refs. [21, 31], is encouraging.

We now turn to the so-called trace anomaly, $\varepsilon-3p$. The expectation value

$$-\frac{4}{T^4}c_2(t)\left\langle G^a_{\mu\nu}(t,x)G^a_{\mu\nu}(t,x)\right\rangle, \tag{4.2}$$

as a function of tT^2 is plotted in Fig. 4 for $T/T_c=1.68$. (Results for other temperatures are deferred to Appendix A). As we noted, the two-loop order (N^{2}LO) and the three-loop order (N^{3}LO) coefficients are available for the trace anomaly. We observe that, already with the N^{2}LO coefficient, the continuum limit (the gray band) is almost constant in t within our fit ranges. Thus, naturally, the extrapolation of the continuum limit to $t=0$ is quite insensitive on the choices N^{2}LO or N^{3}LO, and $\mu=\mu_0(t)$ or $\mu=\mu_d(t)$. Similarly to the entropy density above, for N^{2}LO, we use the extrapolation of the form (3.10), (the results with the linear t extrapolation in the N^{2}LO is given by Ref. [14] (FlowQCD 2016)), while for the N^{3}LO, we used both Eq. (3.10) and the linear t extrapolation. All the results are almost degenerate as also be seen in Fig. 5; as the 4th parentheses in Table 1 shows, however, the use of the N^{3}LO coefficient certainly reduces the dependence on the choice of the renormalization scale.

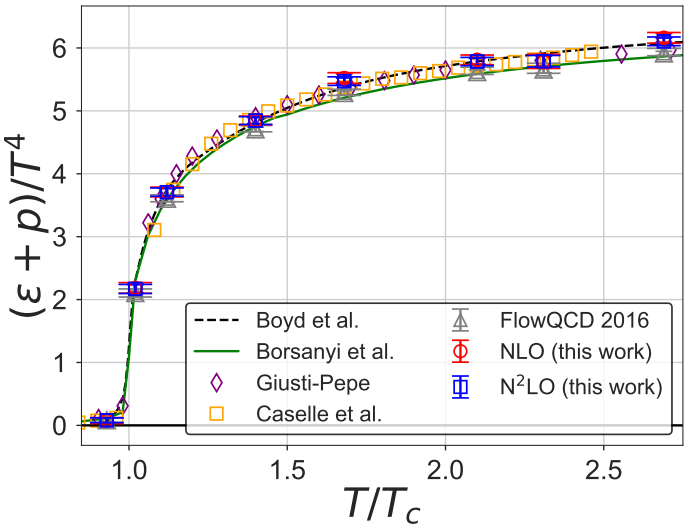

(a)

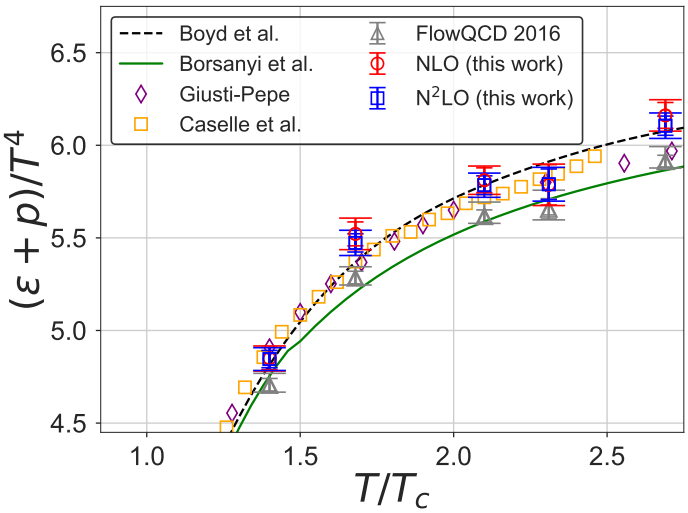

(b)

Fig. 3: Summary of the entropy density as the function of T/T_c. In the lower panel, the region $4.5 \lesssim (\varepsilon + p)/T^4 \lesssim 6.5$ is magnified. The results in the present paper are the red circles (NLO) and the blue squares (N^{2}LO). The error bars are including the systematic error as well as the statistical error; see Table 1 and the main text for details. For comparison, we also plotted the results of Refs. [14, 21, 23, 29, 31].

Acknowledgments

We would like to thank Robert V. Harlander, Kazuyuki Kanaya, Yusuke Taniguchi, and Ryosuke Yanagihara for helpful discussions. This work was supported by JSPS Grant-in-Aid for Scientific Research Grant Numbers, JP17K05442 (M.K.) and JP16H03982 (H.S.). Numerical simulation was carried out on IBM System Blue Gene Solution at KEK under its Large-Scale Simulation Program (No. 16/17-07).

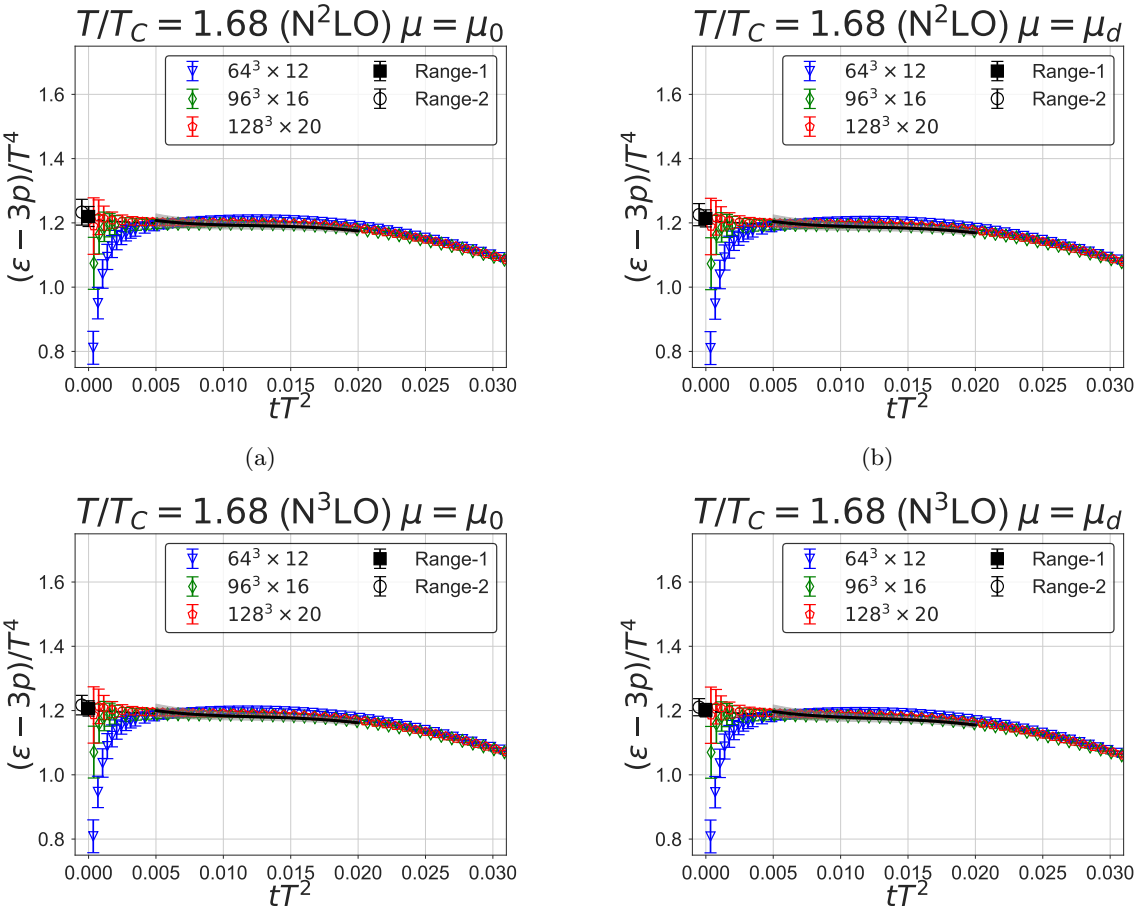

(a) (b) (c) (d)

Fig. 4: Equation (4.2) as the function of tT^2. $T = 1.68T_c$. In each panel, the order of perturbation theory and the choice of the renormalization scale are indicated. The errors are statistical only. The extrapolation of the continuum limit (the gray band) to $t = 0$ is plotted by the black circle (obtained by the fit range (3.14)) and the white circle (obtained by the fit range (3.15)).

A. Numerical results (continued)

In this appendix, we include the plots of Eqs. (4.1) and (4.2) for temperatures $T \neq 1.68T_c$.

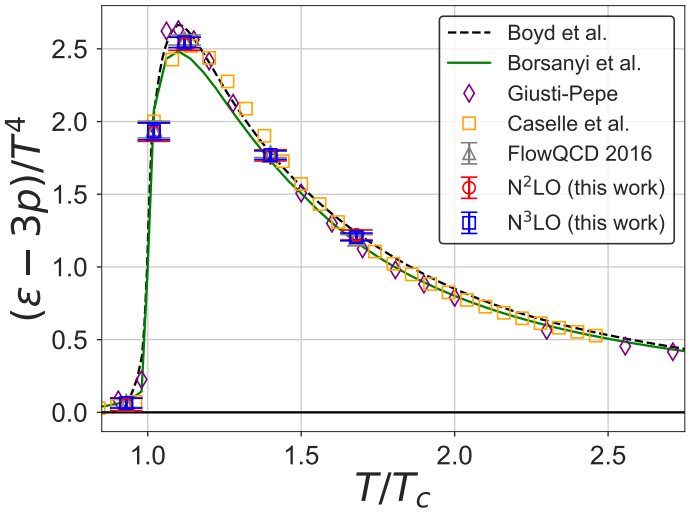

(a)

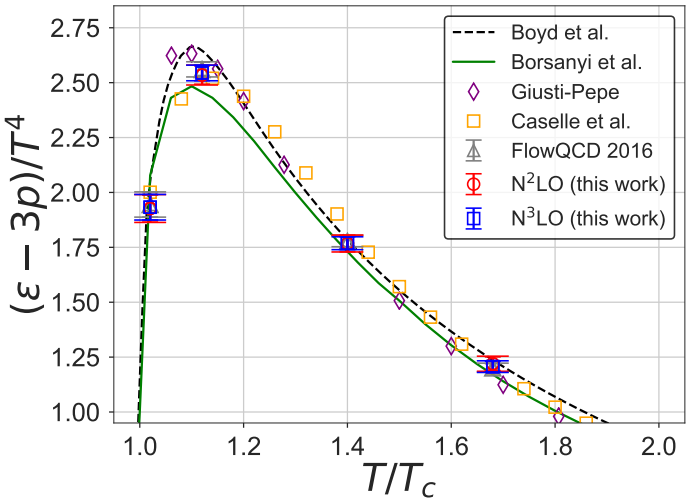

(b)

Fig. 5: Summary of the trace anomaly as the function of T/T_c. In the lower panel, the region $1.00 \lesssim (\varepsilon - 3p)/T^4 \lesssim 2.75$ is magnified. The results in the present paper are the red circles ($\mathrm{N^2LO}$) and the blue squares ($\mathrm{N^3LO}$). The error bars are including the systematic error as well as the statistical error; see Table 1 for details. For comparison, we also plotted the results of Refs. [14, 21, 23, 29, 31].

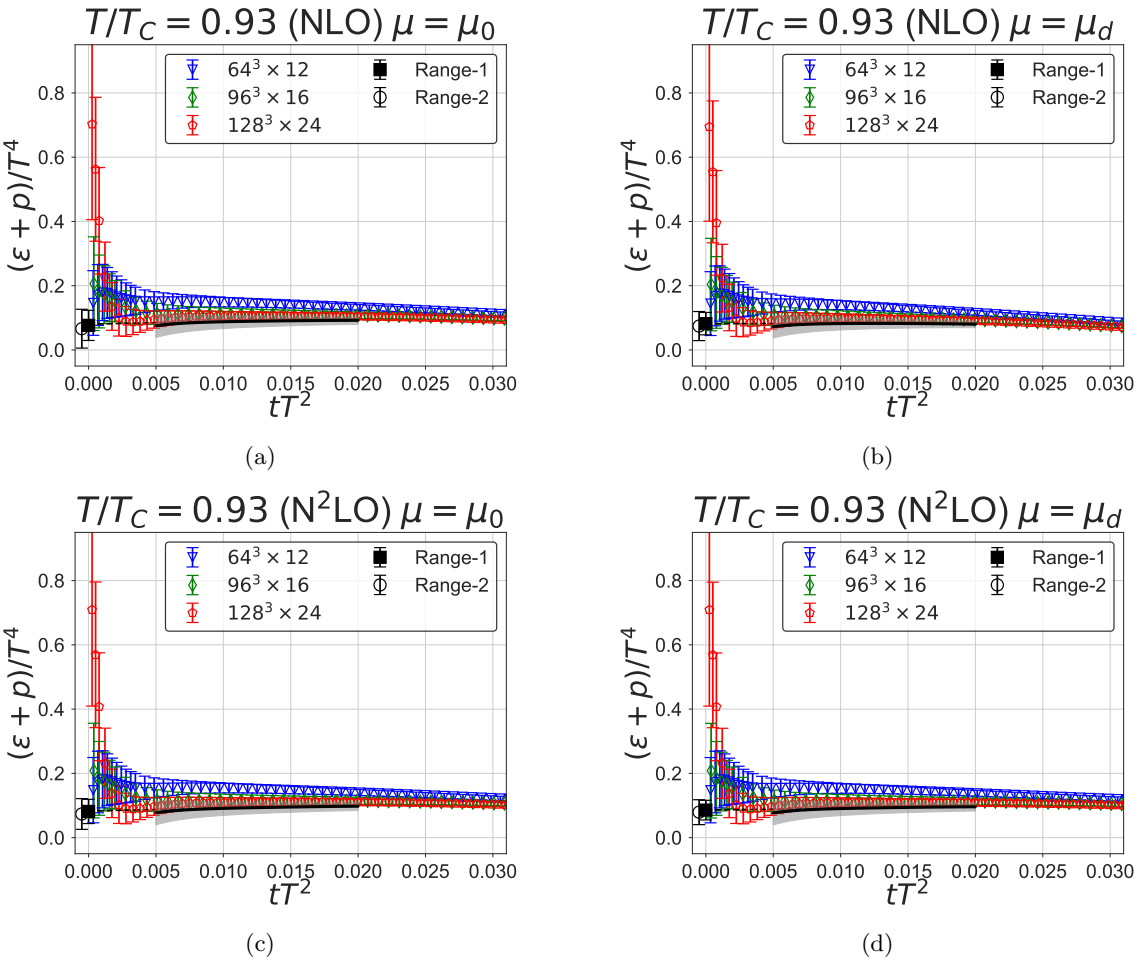

(a) (b) (c) (d)

Fig. A1: Same as Fig. 2. $T = 0.93T_c$.

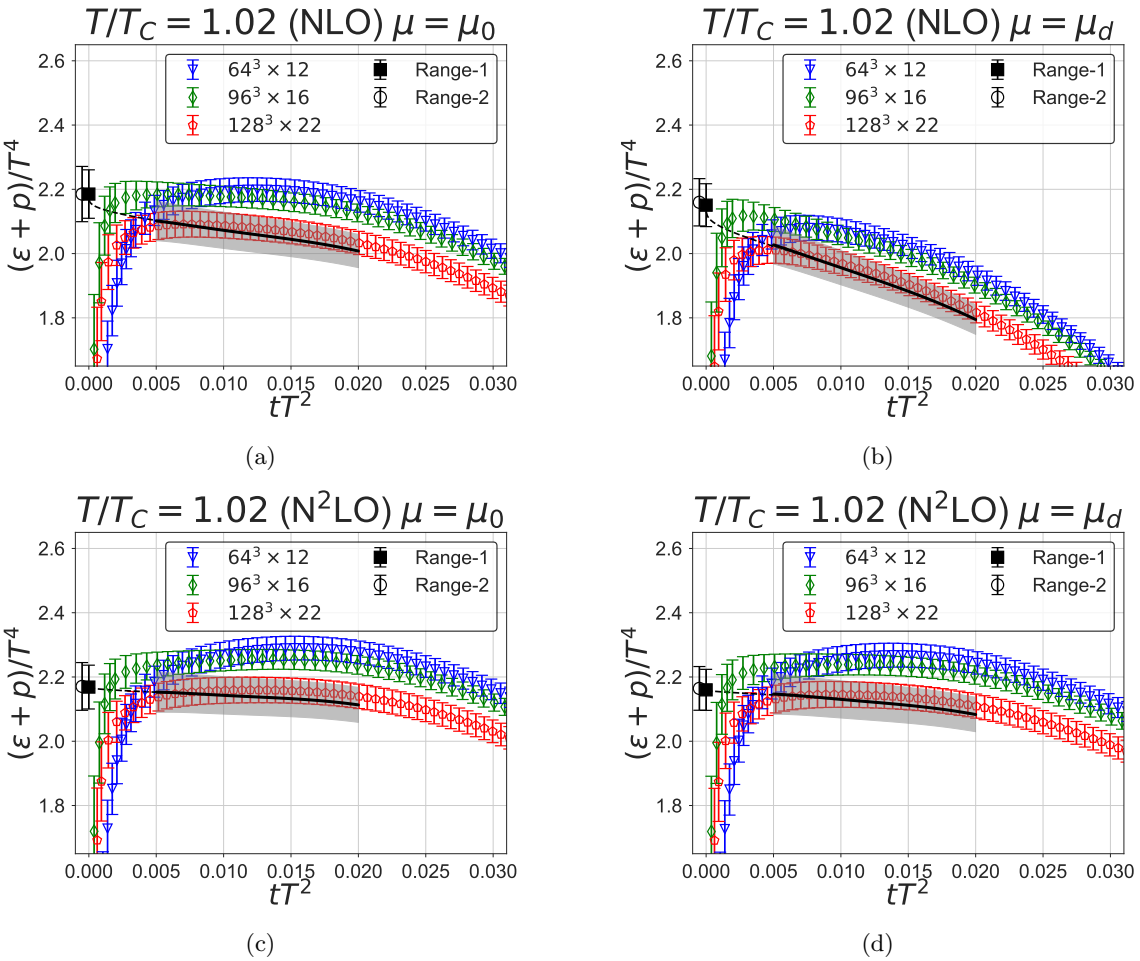

(a) (b) (c) (d)

Fig. A2: Same as Fig. 2. $T = 1.02T_c$.

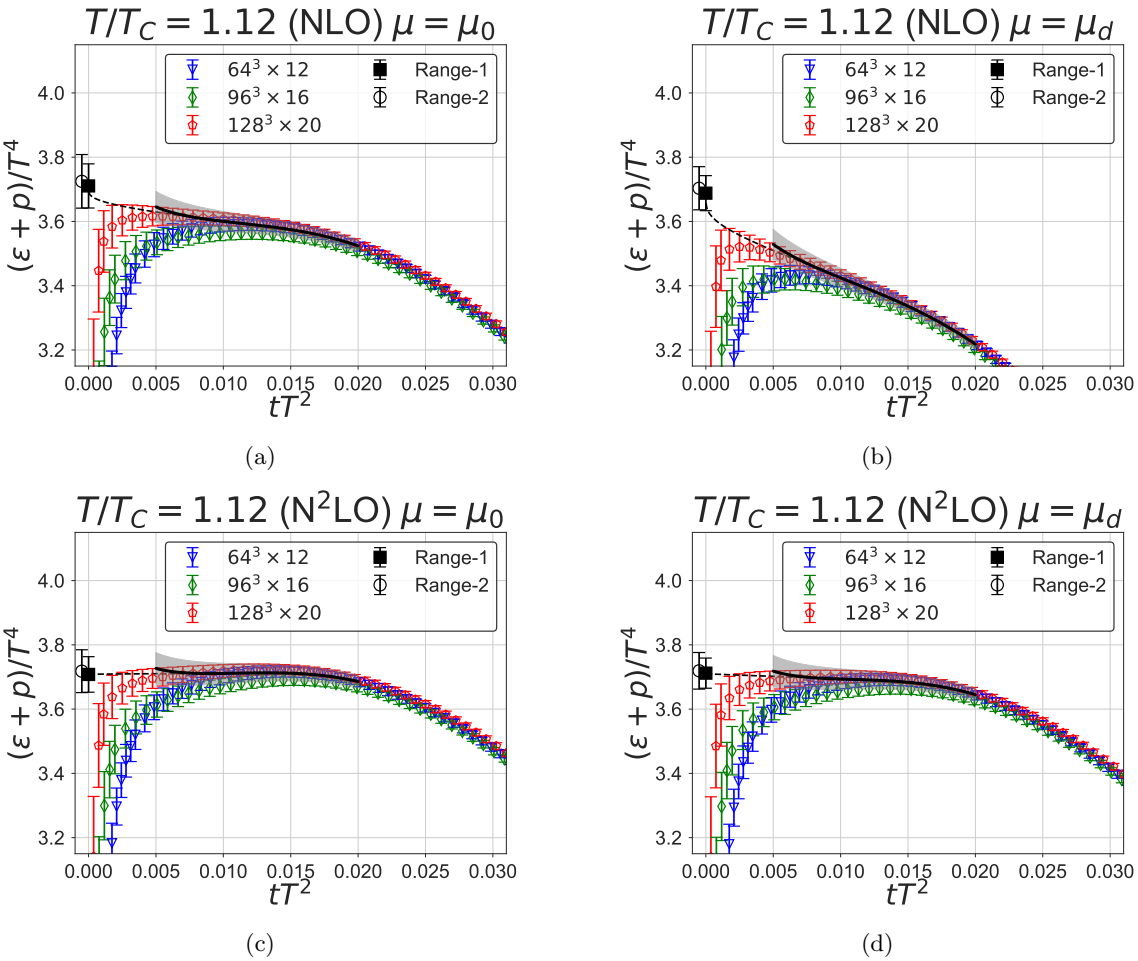

(a) (b) (c) (d)

Fig. A3: Same as Fig. 2. $T = 1.12T_c$.

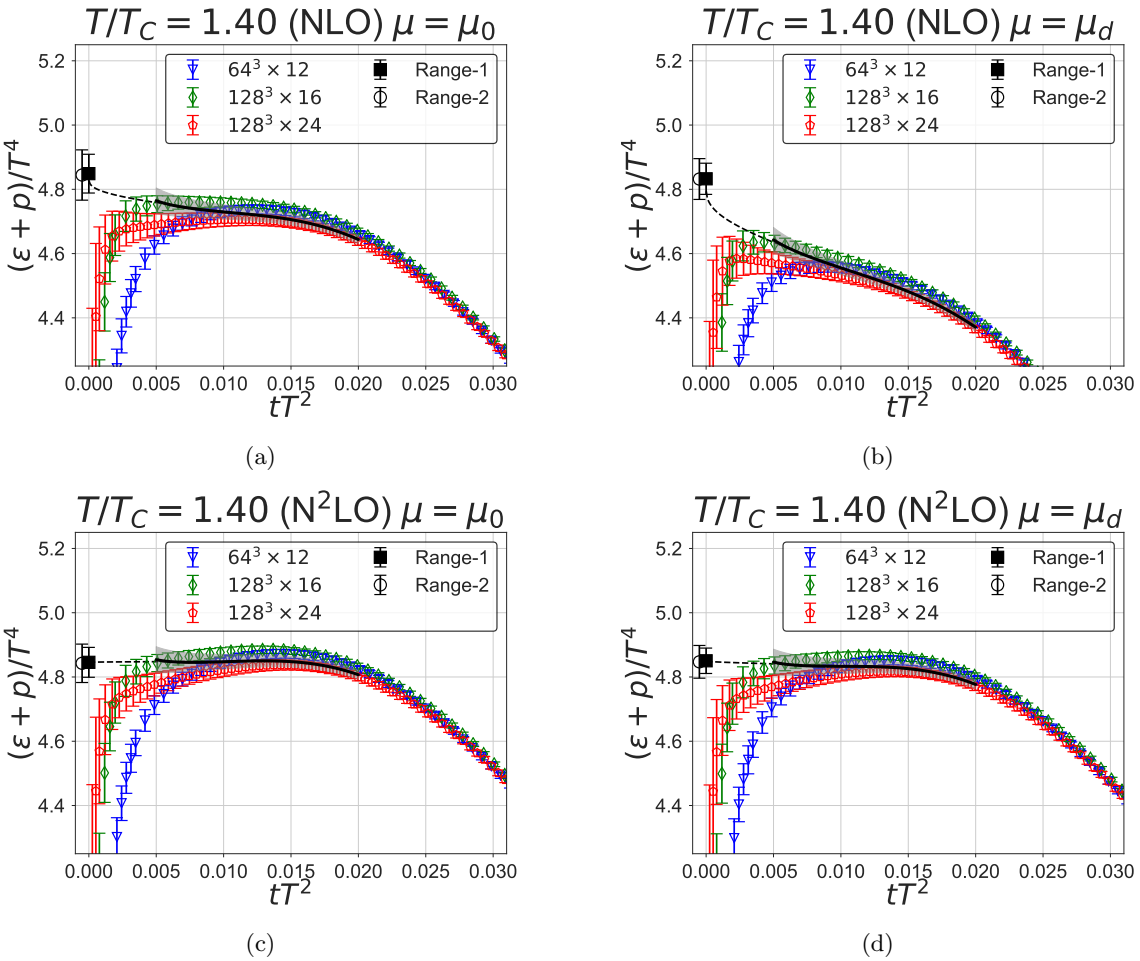

(a) (b) (c) (d)

Fig. A4: Same as Fig. 2. $T = 1.40T_c$.

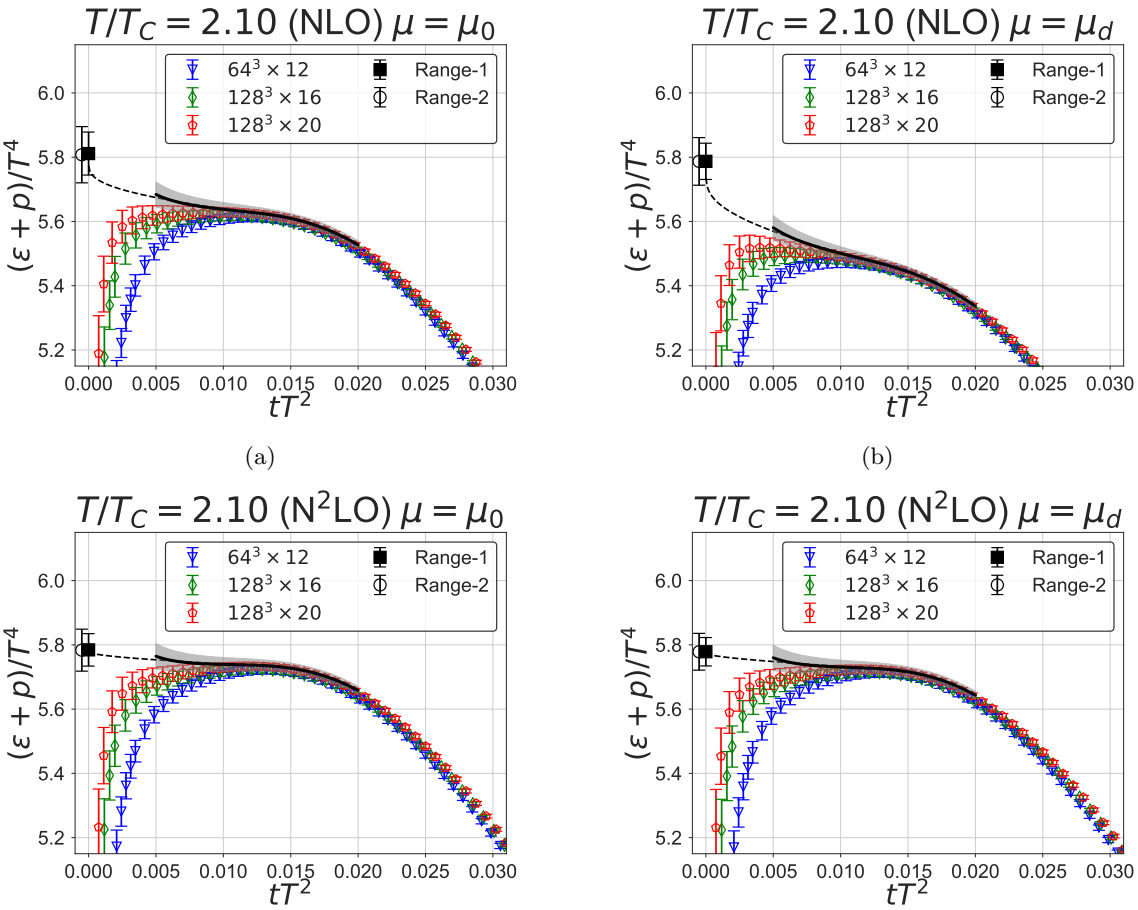

(a) (b) (c) (d)

Fig. A5: Same as Fig. 2. $T = 2.10T_c$.

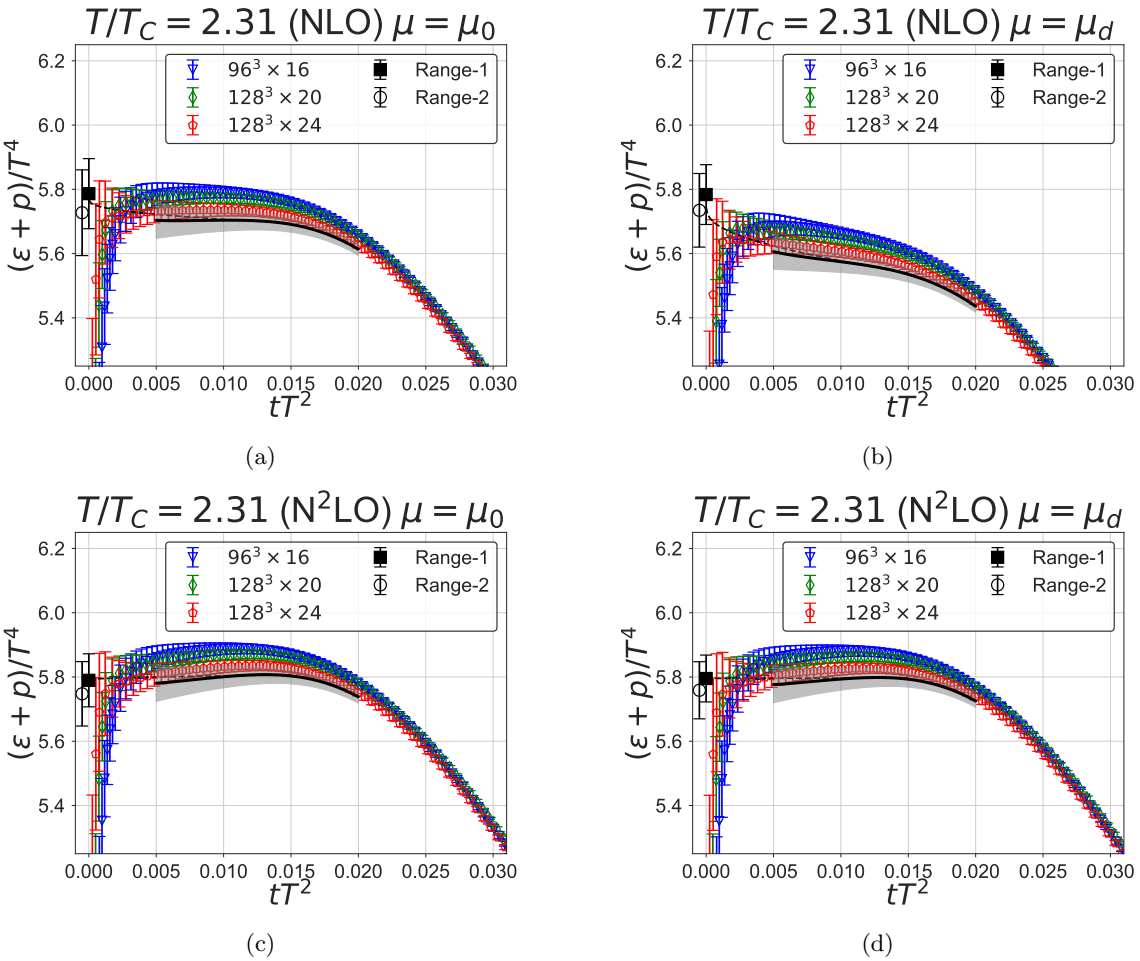

(a) (b) (c) (d)

Fig. A6: Same as Fig. 2. $T = 2.31T_c$.

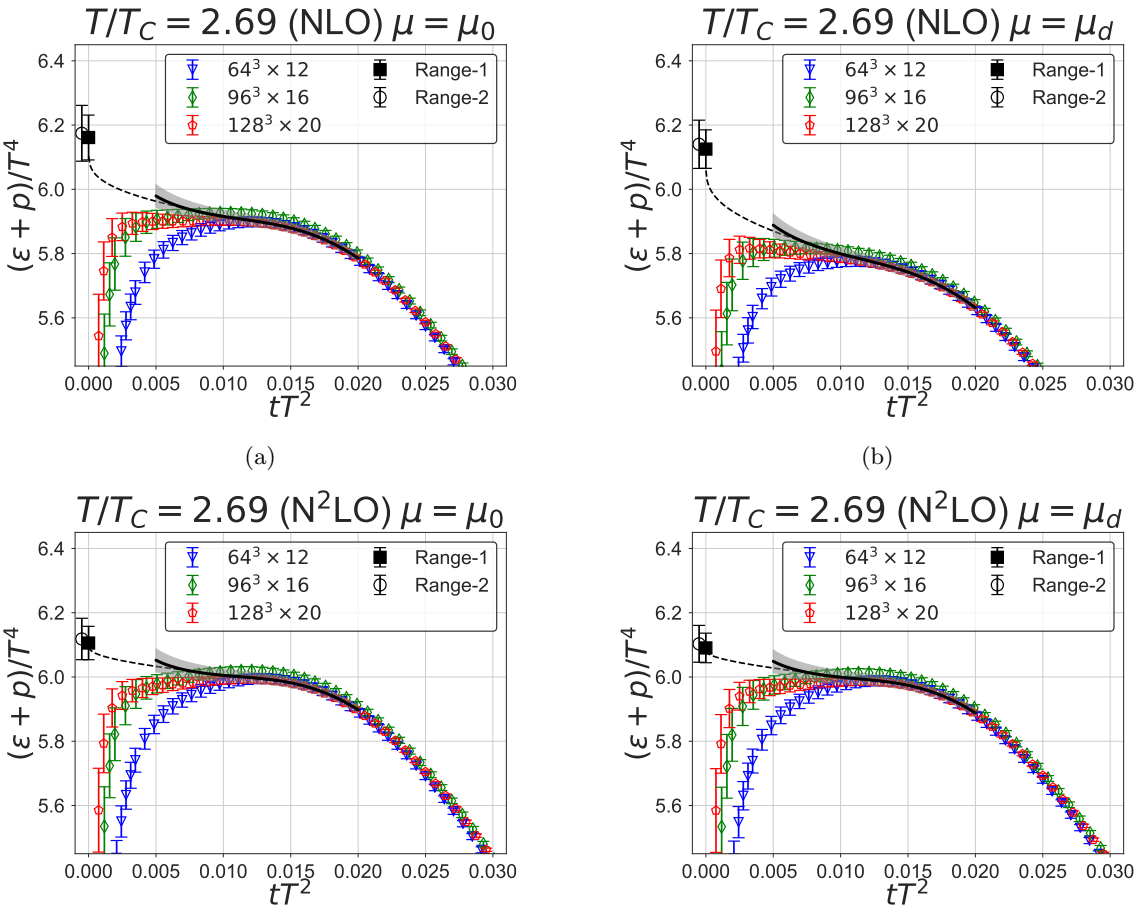

(a) (b)

(c) (d)

Fig. A7: Same as Fig. 2. $T = 2.69T_c$.

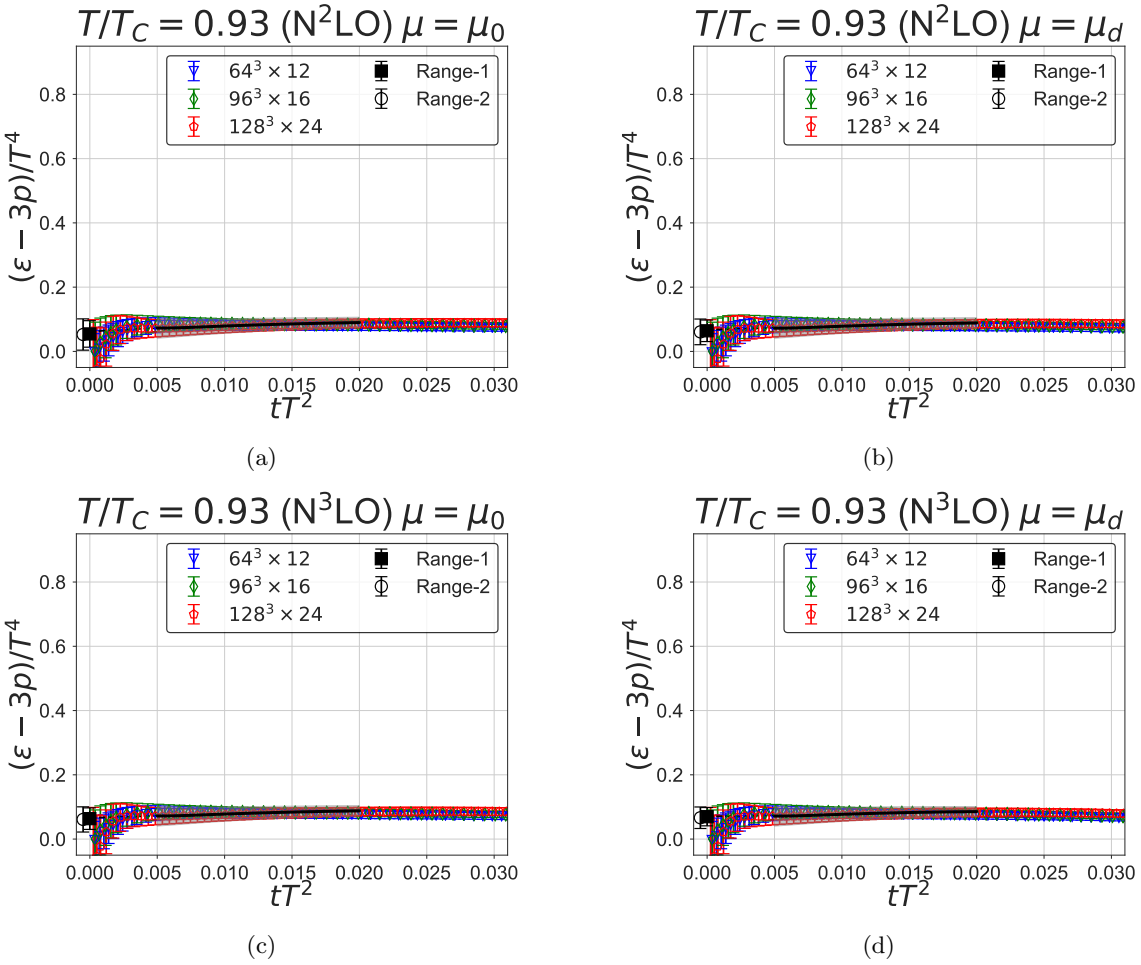

(a) (b) (c) (d)

Fig. A8: Same as Fig. 4. $T = 0.93T_c$.

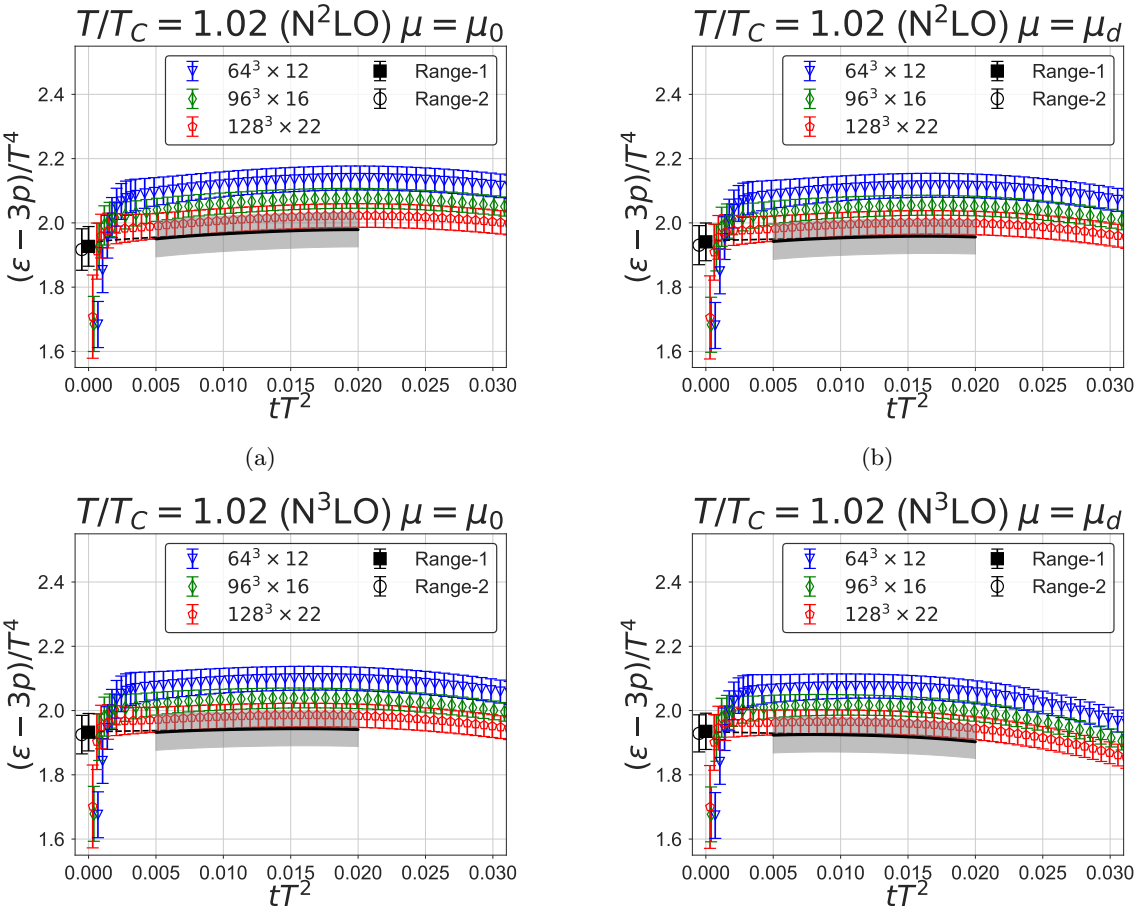

(a) (b)

(c) (d)

Fig. A9: Same as Fig. 4. $T = 1.02T_c$.

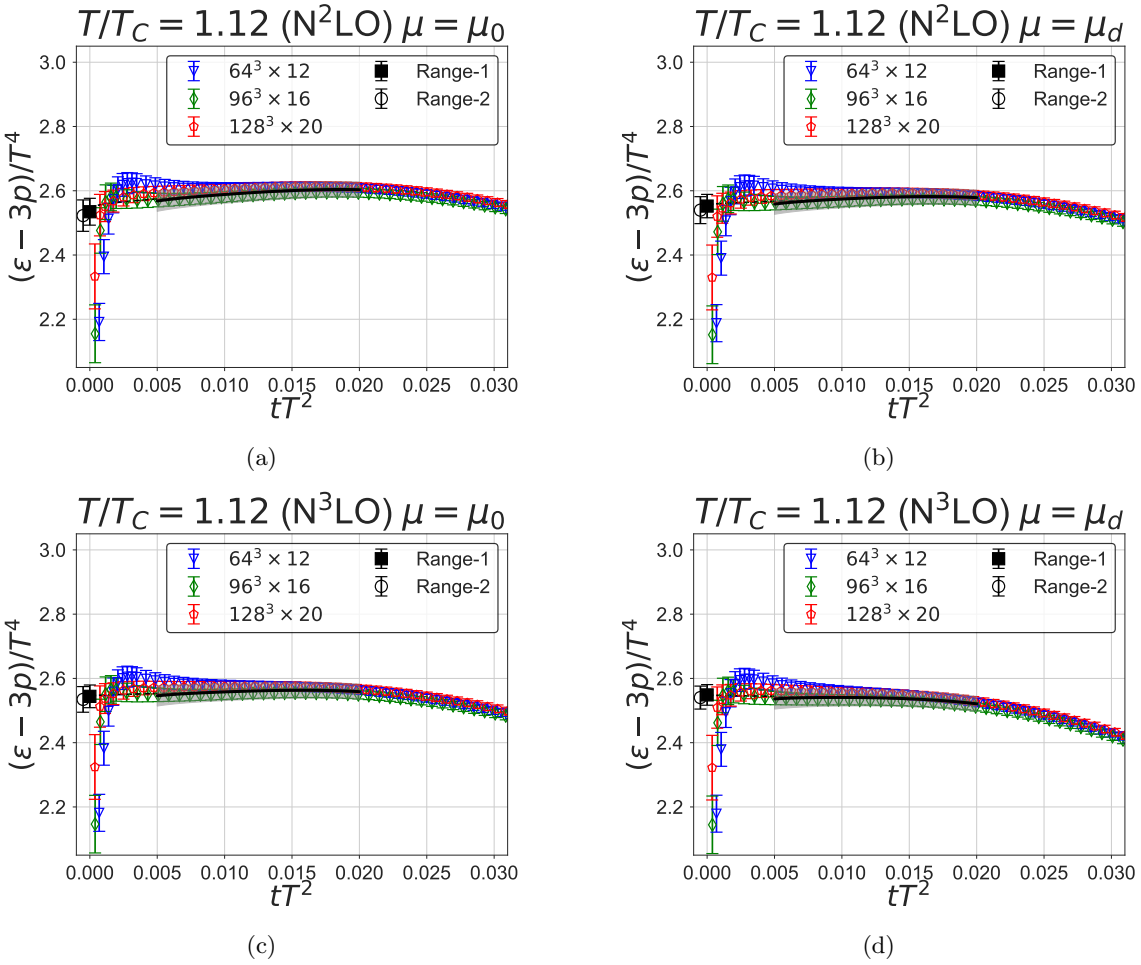

(a) (b)

(c) (d)

Fig. A10: Same as Fig. 4. $T = 1.12T_c$.

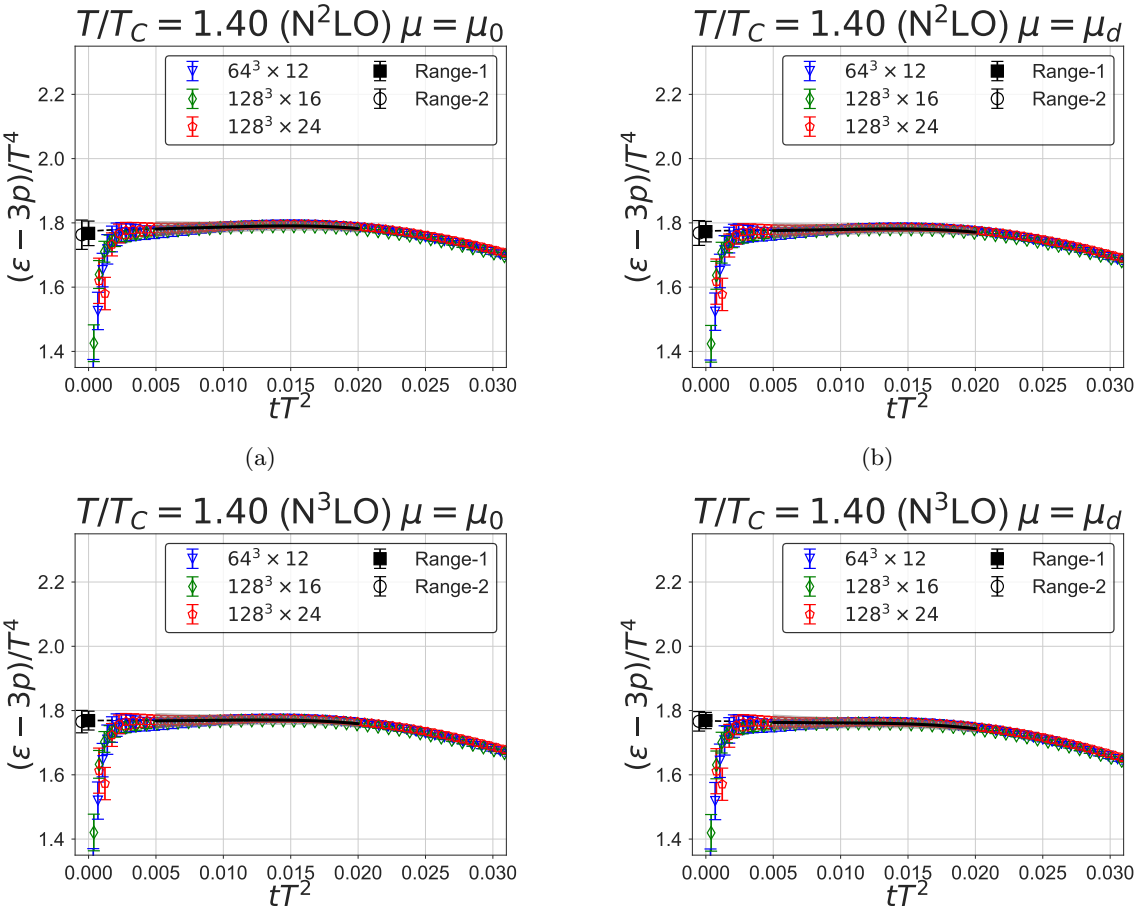

(a) (b)

(c) (d)

Fig. A11: Same as Fig. 4. $T = 1.40T_c$.

References

[1] H. Suzuki, PTEP **2013**, 083B03 (2013) Erratum: [PTEP **2015**, 079201 (2015)] doi:10.1093/ptep/ptt059, 10.1093/ptep/ptv094 [arXiv:1304.0533 [hep-lat]].

[2] H. Makino and H. Suzuki, PTEP **2014**, 063B02 (2014) Erratum: [PTEP **2015**, 079202 (2015)] doi:10.1093/ptep/ptu070, 10.1093/ptep/ptv095 [arXiv:1403.4772 [hep-lat]].

[3] R. Narayanan and H. Neuberger, JHEP **0603**, 064 (2006) doi:10.1088/1126-6708/2006/03/064 [hep-th/0601210].

[4] M. Lüscher, Commun. Math. Phys. **293**, 899 (2010) doi:10.1007/s00220-009-0953-7 [arXiv:0907.5491 [hep-lat]].

[5] M. Lüscher, JHEP **1008**, 071 (2010) Erratum: [JHEP **1403**, 092 (2014)] doi:10.1007/JHEP08(2010)071, 10.1007/JHEP03(2014)092 [arXiv:1006.4518 [hep-lat]].

[6] M. Lüscher and P. Weisz, JHEP **1102**, 051 (2011) doi:10.1007/JHEP02(2011)051 [arXiv:1101.0963 [hep-th]].

[7] M. Lüscher, JHEP **1304**, 123 (2013) doi:10.1007/JHEP04(2013)123 [arXiv:1302.5246 [hep-lat]].

[8] S. Caracciolo, G. Curci, P. Menotti and A. Pelissetto, Annals Phys. **197**, 119 (1990). doi:10.1016/0003-4916(90)90203-Z

[9] H. Suzuki, PoS LATTICE **2016**, 002 (2017) doi:10.22323/1.256.0002 [arXiv:1612.00210 [hep-lat]].

[10] L. Del Debbio, A. Patella and A. Rago, JHEP **1311**, 212 (2013) doi:10.1007/JHEP11(2013)212 [arXiv:1306.1173 [hep-th]].

[11] F. Capponi, A. Rago, L. Del Debbio, S. Ehret and R. Pellegrini, PoS LATTICE **2015**, 306 (2016) doi:10.22323/1.251.0306 [arXiv:1512.02851 [hep-lat]].

[12] M. Asakawa *et al.* [FlowQCD Collaboration], Phys. Rev. D **90**, no. 1, 011501 (2014) Erratum: [Phys. Rev. D **92**, no. 5, 059902 (2015)] doi:10.1103/PhysRevD.90.011501, 10.1103/PhysRevD.92.059902 [arXiv:1312.7492 [hep-lat]].

[13] Y. Taniguchi, S. Ejiri, R. Iwami, K. Kanaya, M. Kitazawa, H. Suzuki, T. Umeda and N. Wakabayashi, Phys. Rev. D **96**, no. 1, 014509 (2017) doi:10.1103/PhysRevD.96.014509 [arXiv:1609.01417 [hep-lat]].

[14] M. Kitazawa, T. Iritani, M. Asakawa, T. Hatsuda and H. Suzuki, Phys. Rev. D **94**, no. 11, 114512 (2016) doi:10.1103/PhysRevD.94.114512 [arXiv:1610.07810 [hep-lat]].

[15] S. Ejiri *et al.*, PoS LATTICE **2016**, 058 (2017) doi:10.22323/1.256.0058 [arXiv:1701.08570 [hep-lat]].

[16] M. Kitazawa, T. Iritani, M. Asakawa and T. Hatsuda, Phys. Rev. D **96**, no. 11, 111502 (2017) doi:10.1103/PhysRevD.96.111502 [arXiv:1708.01415 [hep-lat]].

[17] K. Kanaya *et al.* [WHOT-QCD Collaboration], EPJ Web Conf. **175**, 07023 (2018) doi:10.1051/epjconf/201817507023 [arXiv:1710.10015 [hep-lat]].

[18] Y. Taniguchi *et al.* [WHOT-QCD Collaboration], EPJ Web Conf. **175**, 07013 (2018) doi:10.1051/epjconf/201817507013 [arXiv:1711.02262 [hep-lat]].

[19] R. Yanagihara, T. Iritani, M. Kitazawa, M. Asakawa and T. Hatsuda, arXiv:1803.05656 [hep-lat].

[20] T. Hirakida, E. Itou and H. Kouno, arXiv:1805.07106 [hep-lat].

[21] G. Boyd, J. Engels, F. Karsch, E. Laermann, C. Legeland, M. Lütgemeier and B. Petersson, Nucl. Phys. B **469**, 419 (1996) doi:10.1016/0550-3213(96)00170-8 [hep-lat/9602007].

[22] M. Okamoto *et al.* [CP-PACS Collaboration], Phys. Rev. D **60**, 094510 (1999) doi:10.1103/PhysRevD.60.094510 [hep-lat/9905005].

[23] S. Borsányi, G. Endrődi, Z. Fodor, S. D. Katz and K. K. Szabó, JHEP **1207**, 056 (2012) doi:10.1007/JHEP07(2012)056 [arXiv:1204.6184 [hep-lat]].

[24] S. Borsányi, Z. Fodor, C. Hoelbling, S. D. Katz, S. Krieg and K. K. Szabó, Phys. Lett. B **730**, 99 (2014) doi:10.1016/j.physletb.2014.01.007 [arXiv:1309.5258 [hep-lat]].

[25] A. Bazavov *et al.* [HotQCD Collaboration], Phys. Rev. D **90**, 094503 (2014) doi:10.1103/PhysRevD.90.094503 [arXiv:1407.6387 [hep-lat]].

[26] M. Shirogane, S. Ejiri, R. Iwami, K. Kanaya and M. Kitazawa, Phys. Rev. D **94**, no. 1, 014506 (2016) doi:10.1103/PhysRevD.94.014506 [arXiv:1605.02997 [hep-lat]].

[27] L. Giusti and M. Pepe, Phys. Rev. Lett. **113**, 031601 (2014) doi:10.1103/PhysRevLett.113.031601 [arXiv:1403.0360 [hep-lat]].

[28] L. Giusti and M. Pepe, Phys. Rev. D **91**, 114504 (2015) doi:10.1103/PhysRevD.91.114504 [arXiv:1503.07042 [hep-lat]].

[29] L. Giusti and M. Pepe, Phys. Lett. B **769**, 385 (2017) doi:10.1016/j.physletb.2017.04.001 [arXiv:1612.00265 [hep-lat]].

[30] M. Dalla Brida, L. Giusti and M. Pepe, EPJ Web Conf. **175**, 14012 (2018) doi:10.1051/epjconf/201817514012 [arXiv:1710.09219 [hep-lat]].

[31] M. Caselle, A. Nada and M. Panero, Phys. Rev. D **98**, no. 5, 054513 (2018) doi:10.1103/PhysRevD.98.054513 [arXiv:1801.03110 [hep-lat]].

[32] R. V. Harlander, Y. Kluth and F. Lange, arXiv:1808.09837 [hep-lat].
[33] H. Suzuki, PTEP **2015**, no. 10, 103B03 (2015) doi:10.1093/ptep/ptv139 [arXiv:1507.02360 [hep-lat]].
[34] R. V. Harlander and T. Neumann, JHEP **1606**, 161 (2016) doi:10.1007/JHEP06(2016)161 [arXiv:1606.03756 [hep-ph]].
[35] S. L. Adler, J. C. Collins and A. Duncan, Phys. Rev. D **15**, 1712 (1977). doi:10.1103/PhysRevD.15.1712
[36] N. K. Nielsen, Nucl. Phys. B **120**, 212 (1977). doi:10.1016/0550-3213(77)90040-2
[37] J. C. Collins, A. Duncan and S. D. Joglekar, Phys. Rev. D **16**, 438 (1977). doi:10.1103/PhysRevD.16.438
[38] D. J. Gross and F. Wilczek, Phys. Rev. Lett. **30**, 1343 (1973). doi:10.1103/PhysRevLett.30.1343
[39] H. D. Politzer, Phys. Rev. Lett. **30**, 1346 (1973). doi:10.1103/PhysRevLett.30.1346
[40] W. E. Caswell, Phys. Rev. Lett. **33**, 244 (1974). doi:10.1103/PhysRevLett.33.244
[41] D. R. T. Jones, Nucl. Phys. B **75**, 531 (1974). doi:10.1016/0550-3213(74)90093-5
[42] O. V. Tarasov, A. A. Vladimirov and A. Y. Zharkov, Phys. Lett. **93B**, 429 (1980). doi:10.1016/0370-2693(80)90358-5
[43] S. A. Larin and J. A. M. Vermaseren, Phys. Lett. B **303**, 334 (1993) doi:10.1016/0370-2693(93)91441-O [hep-ph/9302208].
[44] T. van Ritbergen, J. A. M. Vermaseren and S. A. Larin, Phys. Lett. B **400**, 379 (1997) doi:10.1016/S0370-2693(97)00370-5 [hep-ph/9701390].
[45] S. Aoki *et al.*, Eur. Phys. J. C **77**, no. 2, 112 (2017) doi:10.1140/epjc/s10052-016-4509-7 [arXiv:1607.00299 [hep-lat]].
[46] M. Tanabashi *et al.* [Particle Data Group], Phys. Rev. D **98**, no. 3, 030001 (2018). doi:10.1103/PhysRevD.98.030001